



**HAL**  
open science

## Geomorphology of the upper Kalguty Basin, Ukok Plateau, Russian Altai mountains

Philip Deline, Ludovic Ravanel, Jean-Jacques Delannoy, Melaine Le Roy, Vyacheslav I. Molodin, Dimitri V. Cheremisim, Lydia Zotkina, Catherine Cretin, Jean-Michel Geneste, Hugues Plisson

► **To cite this version:**

Philip Deline, Ludovic Ravanel, Jean-Jacques Delannoy, Melaine Le Roy, Vyacheslav I. Molodin, et al.. Geomorphology of the upper Kalguty Basin, Ukok Plateau, Russian Altai mountains. *Journal of Maps*, 2020, 16 (2), pp.595-604. 10.1080/17445647.2020.1800529 . hal-03044345

**HAL Id: hal-03044345**

**<https://hal.science/hal-03044345v1>**

Submitted on 8 Dec 2020

**HAL** is a multi-disciplinary open access archive for the deposit and dissemination of scientific research documents, whether they are published or not. The documents may come from teaching and research institutions in France or abroad, or from public or private research centers.

L'archive ouverte pluridisciplinaire **HAL**, est destinée au dépôt et à la diffusion de documents scientifiques de niveau recherche, publiés ou non, émanant des établissements d'enseignement et de recherche français ou étrangers, des laboratoires publics ou privés.



## Geomorphology of the upper Kalguty Basin, Ukok Plateau, Russian Altai mountains

Philip Deline , Ludovic Ravanel , Jean-Jacques Delannoy , Melaine Le Roy , Vyacheslav I. Molodin , Dimitri V. Cheremisim , Lydia V. Zotkina , Catherine Cretin , Jean-Michel Geneste & Hugues Plisson

To cite this article: Philip Deline , Ludovic Ravanel , Jean-Jacques Delannoy , Melaine Le Roy , Vyacheslav I. Molodin , Dimitri V. Cheremisim , Lydia V. Zotkina , Catherine Cretin , Jean-Michel Geneste & Hugues Plisson (2020) Geomorphology of the upper Kalguty Basin, Ukok Plateau, Russian Altai mountains, Journal of Maps, 16:2, 595-604, DOI: [10.1080/17445647.2020.1800529](https://doi.org/10.1080/17445647.2020.1800529)

To link to this article: <https://doi.org/10.1080/17445647.2020.1800529>



© 2020 The Author(s). Published by Informa UK Limited, trading as Taylor & Francis Group on behalf of Journal of Maps



[View supplementary material](#)



Published online: 14 Aug 2020.



[Submit your article to this journal](#)



Article views: 387



[View related articles](#)



[View Crossmark data](#)



## Geomorphology of the upper Kalguty Basin, Ukok Plateau, Russian Altai mountains

Philip Deline<sup>a</sup>, Ludovic Ravanel<sup>a</sup>, Jean-Jacques Delannoy<sup>a</sup>, Melaine Le Roy<sup>a</sup>, Vyacheslav I. Molodin<sup>b,c</sup>, Dimitri V. Cheremisim<sup>b,c</sup>, Lydia V. Zotkina<sup>b,c</sup>, Catherine Cretin<sup>d</sup>, Jean-Michel Geneste<sup>d</sup> and Hugues Plisson<sup>d</sup>

<sup>a</sup>Université Savoie Mont Blanc, CNRS, EDYTEM, Chambéry, France; <sup>b</sup>Institute of Archeology and Ethnography of the Siberian Branch of the Russian Academy of Sciences, Novosibirsk, Russia; <sup>c</sup>Novosibirsk State University, Novosibirsk, Russia; <sup>d</sup>Université de Bordeaux, CNRS, Ministère de la Culture et de la Communication, PACEA, Pessac, France

### ABSTRACT

As part of an archaeological research project, we investigate the geomorphology of the cold and arid study area by combining field mapping with use of orthoimages and DEM. To the north of a broad trunk valley floor, gentle slopes continuously vegetated culminate around 3000 m, while to the south steep slopes reaching to 3500 m are deeply incised and covered mainly by regolith. The basin has been intensively glaciated as evidenced by the till covering the gentler slopes, several morainic complexes, kame terraces and roches moutonnées. The present morphodynamics of this permafrost-affected basin is mainly periglacial, with blockfields, solifluction lobes, patterned ground and rock glaciers on gentle slopes to high-elevated flat terrain, and block slopes and rockfall talus on steeper slopes. Large alluvial fans at the outlet of the steep lateral valleys constrain the anastomosing channel of the Kalguty river. Active braided channels in those valleys evidence seasonal high peak discharge.

### ARTICLE HISTORY

Received 12 March 2020  
Revised 26 May 2020  
Accepted 15 July 2020

### KEYWORDS

Glacial and periglacial geomorphology; geomorphological mapping; Ukok Plateau; Altai mountains

## 1. Introduction

The present study was motivated by ongoing archaeological research that began in 1990 on the Ukok Plateau (Molodin et al., 2004), a border region with Kazakhstan, China, and Mongolia that is bounded by steep, high-elevated mountain ranges (Figure 1). Ukok, one of the three areas of the ‘Golden Mountains of Altai’ (UNESCO World Heritage region since 1998) is well-known to archaeologists for its *kurgans*, i.e. frozen burial complexes of the 750–250 BCE Pazyryk Culture with mummies like the ‘Ukok Princess’ (Chikisheva et al., 2015). Numerous petroglyph sites are also characteristic of the Ukok Plateau but are difficult to date given the absence of stratigraphy (Molodin & Cheremisim, 2007).

Our multidisciplinary research project aims to place these petroglyphs in their environmental, temporal, and technical contexts. To address the first two objectives, we carried out a detailed geomorphological study of the upper Kalguty basin in order to establish a relative chronology of its morphodynamics since the LGM, as the petroglyph site considered as the oldest in the Ukok, Kalgutinski Rudnik, is located there (Molodin & Cheremisim, 2007). While Pleistocene glacial superfloods (e.g. Rudoy, 2002) or present glacier dynamics (e.g. Ganiushkin et al., 2017) have been intensely studied in the Russian Altai mountains, no detailed geomorphic analysis is available for the Ukok area. This study of the upper

Kalguty basin provides the context for ongoing dating of Pleistocene glacier advances and inferring palaeoclimate from mass balance reconstruction, with the aim to better constrain the age of the rock carvings and the environmental conditions prevailing at that time.

## 2. Geographical, geological and climatic setting

The highest hills to the north of the upper Kalguty basin culminate slightly above 3000 m asl, while the crest-line of the west end of the Saylyugem Range forming the Mongolia/Russia boundary is broadly above 3000 m with a relief reaching > 1000 m, and culminates with the Tundu-Uqgar (3529 m asl; Figure 2). The valley floor drained by the Kalguty river descends from 3000 to 2300 m over a distance of 22 km, the lower half section being 1–1.5 km wide (Figure 3). A continuous alpine meadow with shrub patches extends up to the top of the hills north to the Kalguty river, and to 2700–2800 m to the south.

Devonian volcanogenic sedimentary rocks are dominant in the Saylyugem Range: conglomerates, sandstones, schists, and quartzites, interbedded with marlstones and acid volcanic rocks. Further north, acid (e.g. rhyolite) and basic volcanic rocks are interbedded with sandstones and schists. A N120° fault crosses both formations, while the two small valleys

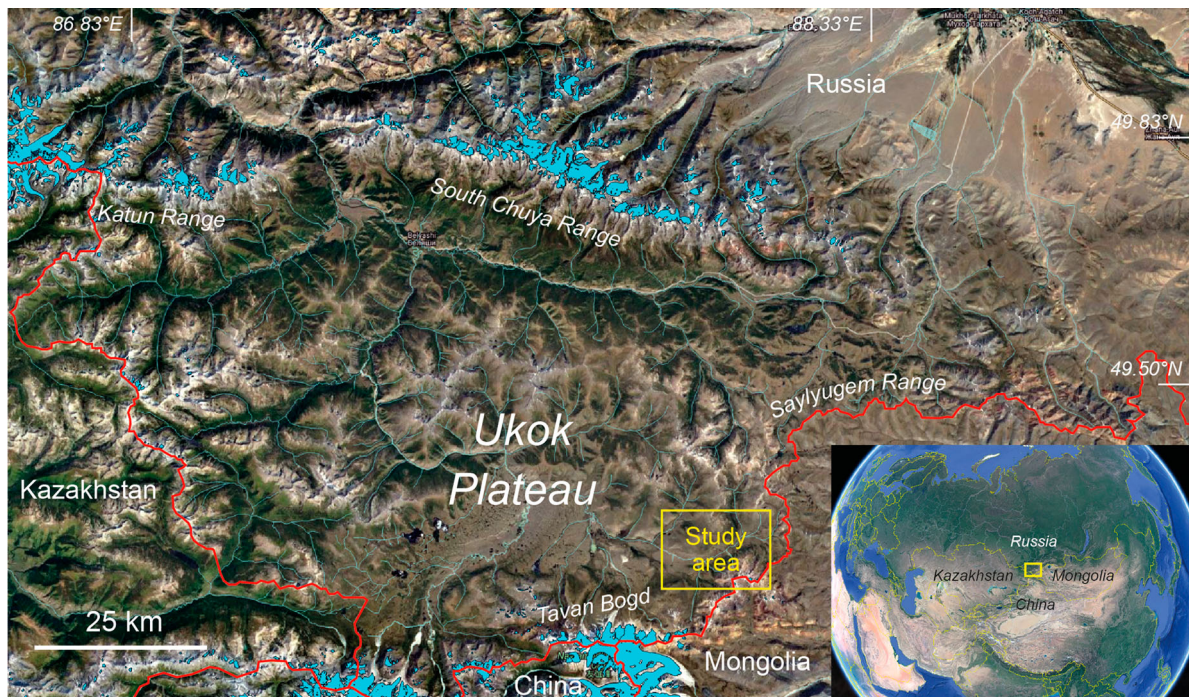


**Figure 1.** Location of the upper Kalguty basin (study area) in the south-east of the Ukok Plateau, Russian Altai Mountains (Google Earth images); blue areas: present-day glacier extent according to RGI (Randolph Glacier Inventory) Consortium (2017); red line: boundaries between Russia, Mongolia, China and Kazakhstan.

north of the Ulan-Dawa river correspond to secondary faults striking N10–40°.

The climate of this arid area of the Altai is cold desert type BWk according to Köppen-Geiger climate classification (Peel et al., 2007): mean annual air temperature is generally negative, e.g.  $-8.3^{\circ}\text{C}$  at Bertek (2250 m asl); annual precipitation decreases from 500 mm in the NW to 100 mm along the border with Mongolia, of which c. 65% occurs in summer (Batbaatar et al., 2018; Shahgedanova et al., 2010).

Two small glaciers are still present at the head of the East valley (RGI Consortium, 2017) with a total area of 0.25 km<sup>2</sup> (Figure 2). Spatial modelling of permafrost in the Altai Mountains (Riseborough et al., 2010) suggests that continuous permafrost (i.e.  $\geq 90\%$  of the area) characterizes the slopes of the study area, whereas sporadic permafrost (10–50%) is present in the valley bottom (Marchenko et al., 2006).

### 3. Geomorphological mapping

A multi-method mapping approach was used (Chandler et al., 2018). Representative areas of the sides and valleys of the upper Kalguty basin were mapped in the field at large scale in July 2015 using a 10 m-contour interval topographic map produced from the SRTM 30 m-DEM, and low-resolution orthoimages from Google Earth (access to East valley, along the boundary with Mongolia, was not authorized by the Russian border police). The hand-drawn maps allowed us to later remotely map the whole study area in detail, using satellite images.

To support the final detailed geomorphological mapping, a high-resolution DEM was built from SPOT6/7 stereo images acquired in 2017, after radiometric corrections (L1A process level). Within Geomatica OrthoEngine (PCI Geomatics), (i) raw images were converted into epipolar pairs, (ii) DEMs were extracted from the overlap between the epipolar pairs (image correlation), and (iii) the epipolar DEMs were geocoded and stitched together to form a 4 m-DEM (triangulation). Two Pléiades panchromatic orthoimages from 18th September 2016 covering the study area (except its most downstream part) were also used for mapping.

Hand-drawn maps were georeferenced in GIS software (QGIS), where detailed geomorphological mapping was carried out using the high-resolution SPOT DEM and Pléiades orthoimages. Despite their uneven quality, colour orthoimages from Google Earth and Bing Maps Aerial were also used through Web Map Service.

### 4. Geomorphic analysis

The study area has been shaped by Pleistocene glaciations but heavily affected later by the post-glacial morphodynamics, mainly periglacial processes. There is a sharp morphological contrast between the gentle slope of hills that form the north side of the valley, likely fully covered by the glacier at its maximal extent, and the steeper Saylyugem Range where crest towers 1000 m above the Kalguty river, with cirques and valleys deeply incised by past mountain glaciers (Main Map; Figure 3).

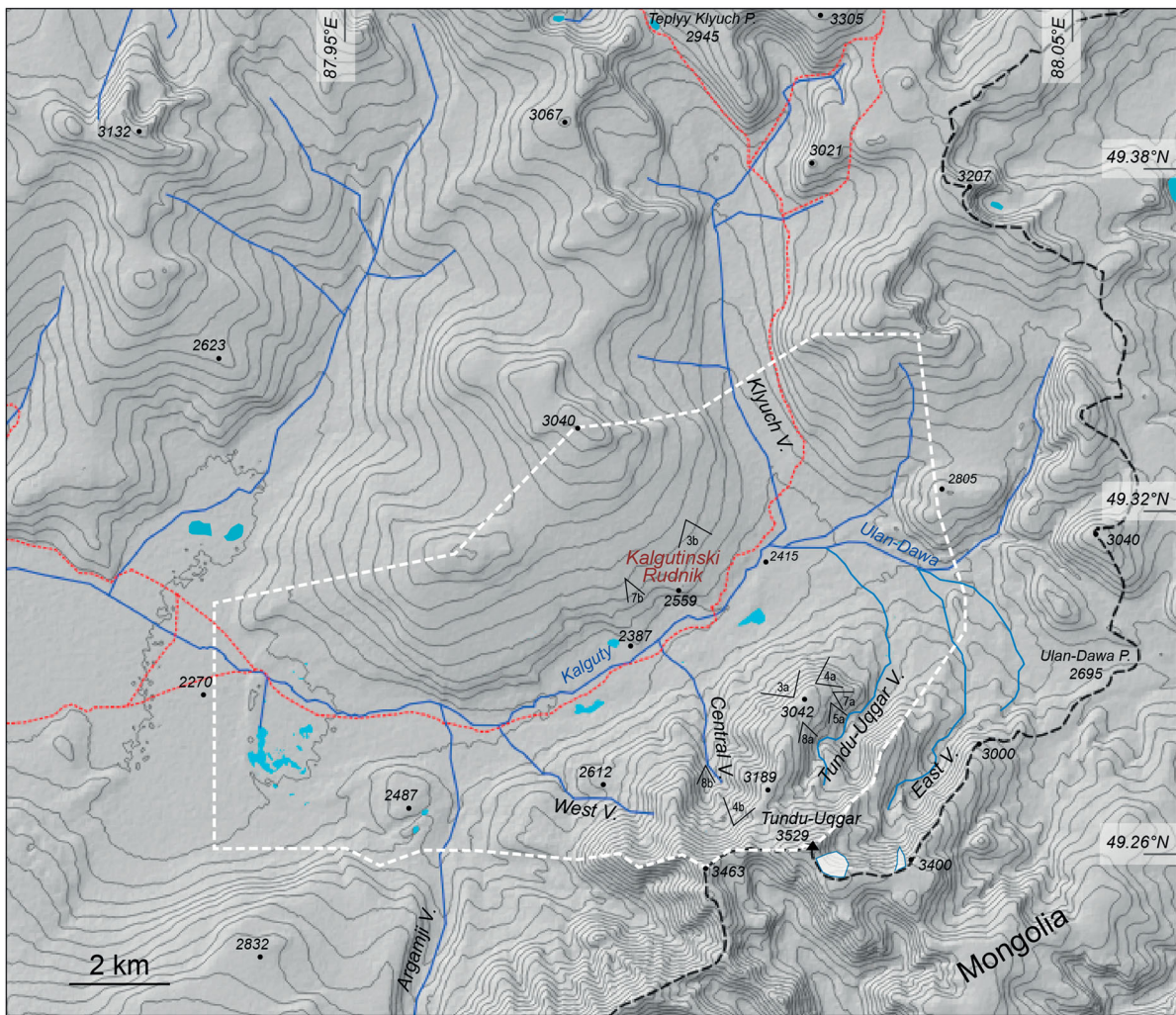


**Figure 2.** Upper Kalguty basin, South-eastern Ukok Plateau. White-dashed polygon: study area; V: valley; P.: pass; white polygons: glaciers (RGI Consortium, 2017); red-dotted line: 4 wheel-drive trails; black-dashed line: boundary along the Saylyugem Range; direction of photos corresponding to figures is indicated; contour interval: 50 m. Topographic map from ASTER GDEM.

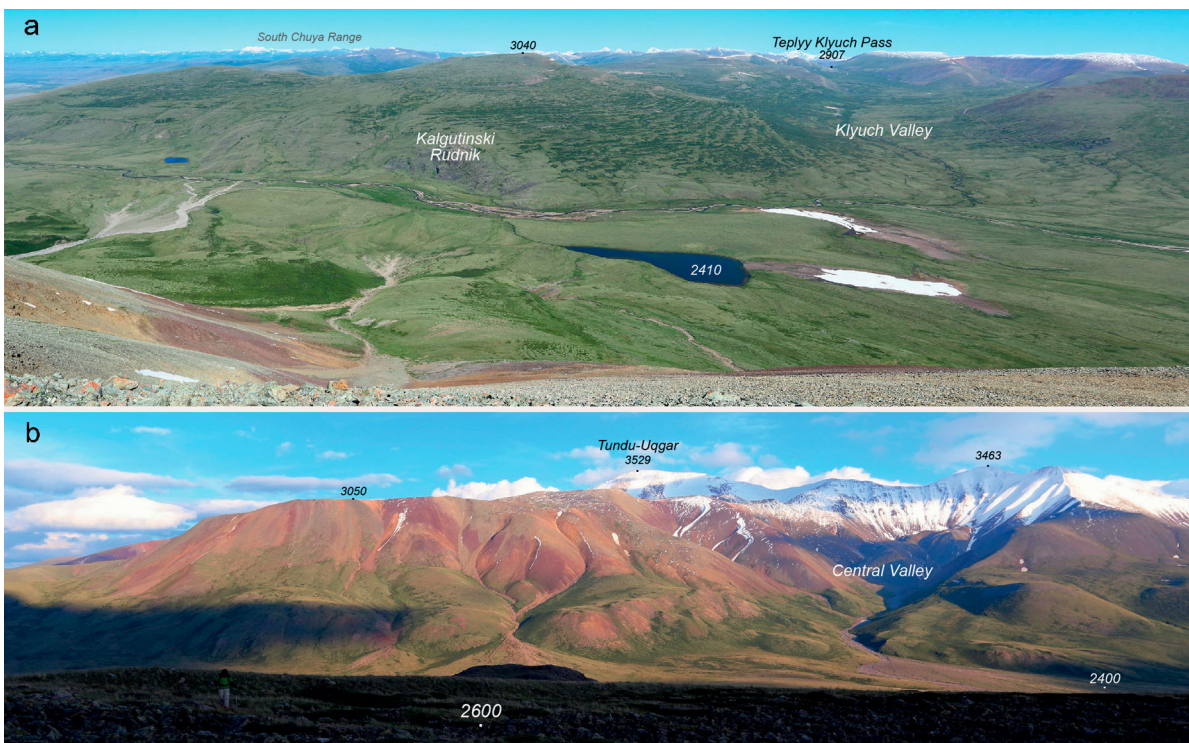


**Figure 3.** The upper Kalguty basin, south-eastern Ukok Plateau, Russian Altai. (a) View to the north. Snow on the South Chuya Range at the horizon. (b) View to the south. The Tundu-Uqgar Valley is deeply incised behind the c. 3050 m plateau. Elevations in m asl.

#### 4.1. Glacial landforms and deposits

A large set of two to six frontal moraines up to 25 m high crosses the Kalguty Valley at c. 2300 m asl, at the western end of the study area. This morainic loop is extended upstream by latero-frontal moraines on both sides of the valley, and by two c. 5-km-long narrow kame terraces on the north side. Upstream from the confluence of Argamji and Kalguty rivers, many small recessional moraines are present at the foot of both valley sides. Striae on asymmetric scoured bedrock at the foot of the north side indicate roches moutonnées, on which numerous erratic boulders were deposited. The main surface of the valley's north side is covered by tills, with few small moraines and kame terraces distributed between c. 2650 and 2920 m asl.

A second morainic complex composed of nested latero-frontal ridges crosses the Klyuch Valley (Figure 3(a)), both sides of which are covered by tills; small moraines are present between this complex and Kalgutinski Rudnik. Downstream from the Tundu-Uqgar Valley, a morainic complex develops from 2480 to 2620 m asl, with erratic boulders on recessional moraines in its upper half (Figure 4(a)); a small morainic arc at c. 3000 m has been built by a former glacier that was partly fed by snow avalanches. The Central Valley morainic complex is better preserved on the right side of the valley, where the glacier front elevation oscillated from 2410 to 2600 m as suggested by the innermost recessional moraine crest; two latero-frontal moraines at 2850 and 3000 m suggest that the

corresponding glacier front was bi-lobate (Figure 4 (b)). Finally, two other morainic complexes are present in the lower part of the Argamji and East Valleys (Main Map); as these moraines are located outside of the study area (Figure 2), we only mapped their crests by remote sensing.

#### 4.2. Periglacial processes and landforms

South of the Kalguty river, slopes are mainly covered by regolith: fine to bouldery blockfields on gentle slopes to high-elevated flat terrain, block slopes and rockfall talus on steeper slopes (Figure 5(a)).

Scree deposits which compose rockfall talus result from freeze–thaw cycles that affect rock outcrops by frost weathering (Figure 5(c)). Fractured rock is cracked by ice segregation when water migration with freezing supplies ice lenses, and secondarily by volumetric expansion in water-filled joints and hydro-fracturing (Matsuoka & Murton, 2008; Murton et al., 2006). Once ice thaws or warms, debris and rock falls accumulate these clasts as talus sheets (Figure 5(a)) or talus cones (Figure 5(b)). Post-depositional redistribution and sorting processes (debris-saturated flow, dry grain flow, supranival sliding of debris) allow the enlargement and stratification of these scree slopes (Sass & Krautblatter, 2007).

Blockfields on gentle slopes – termed block slopes on steeper areas (Washburn, 1973) – form during the Pleistocene by a combination of stripping of a Neogene saprolite (i.e. chemically weathered rock) and

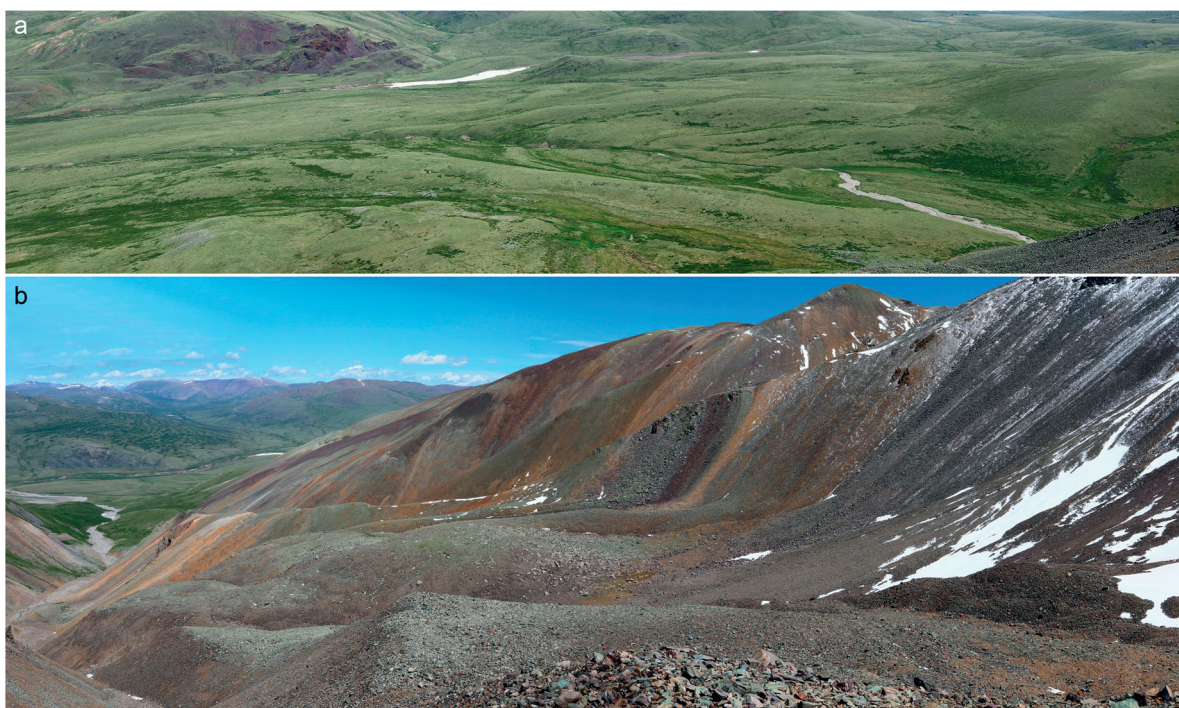


**Figure 4.** (a) Morainic complex downstream from the Tundu-Uqgar Valley (view to the NE). Wide valley drained by the Ulan-Dawa river in the background. (b) Possible right-lateral moraines, and rock glacier complex in the Central cirque between 2850 and 3050 m asl (view to the north). Kalgutinski Rudnik in the left background, at the bottom of the opposite side of the main valley.

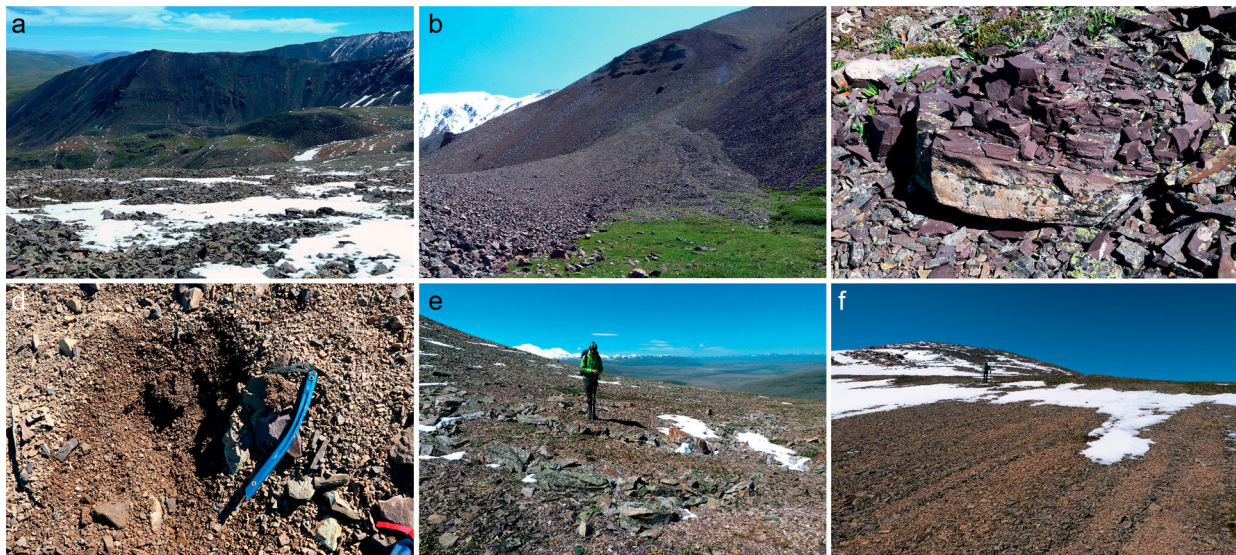


**Figure 5** Regolith landforms resulting from frost weathering and heaving on the 3050 m plateau (except b). (a) Openwork blockfield in the foreground, talus sheets on east side of Tundu-Uqgar Valley in the background; (b) talus cone reworked by debris flows and snow avalanches, block slopes on the right (Central Valley); (c) frost shattering on a c. 50-cm-long rhyolite outcrop; (d) diamictic blockfield, frozen from a depth of c. 15 cm (note a piece of frozen debris close under the ice axe pick); (e) sorted circles; (f) sorted stripes.

frost wedging at the weathering front in pre-existing cracks of the bedrock (Ballantyne, 2010). In a regolith enriched in fines derived by granular disaggregation of clasts (Figure 5(d)) with a <1- to 5-m-thick active layer, ice segregation generates frost heaving; upfreezing and ejection of stones result in a sorting effect with possible formation of patterned ground. Some large sorted circles are present on flat areas (Figure 5(e)), while sorted stripes form on gentle slopes (Figure 5(f)). Quaternary glaciations would generally have changed the regolith little as glaciers were cold-based; after deglaciation, the blockfields have been affected by comminution of clasts by freeze-thaw weathering and removal of fines by wind and surface wash (Ballantyne, 2010). As coarse debris on slopes acts as a ‘thermal semi-conductor’ with a chimney effect (Guodong et al., 2007), mean annual temperature inside the blockfields can be 2.5–4.0°C lower than in adjacent fine-grained regolith (Gorbu-nov et al., 2004).

Patterned ground is well developed on the valley bottom, where high moisture in summer is evidenced by stream channels, peat bogs, and marshes and lakes. Ice wedge polygons, high-centered, likely epigenetic and secondary (Mackay, 1974, 1990) have mainly formed east of the Central Valley fan in till deposits at the base of the south sides of the Kalguty and Ulan-Dawa Valleys, and secondarily in alluvial deposits. These < 15-m-wide polygons are characteristic of permafrost-affected ground: its thermal contraction during cold winters generates repeated vertical cracks in which water from snowmelt, precipitation, flood-water, or active layer water table, enters and allows ice-wedge formation (Black, 1976; Lachenbruch,

1962). Troughs that formed above ice wedges can be infilled by water (Figure 6(a)). However, some narrow > 10 m-long ground cracks located inside the Klyuch morainic complex could result from seasonal frost cracking (Ballantyne, 2018, p. 91), because they seem to be unrelated to the ice-wedge polygons (Figure 6(c)). Finally, patterned ground is also extensively distributed on gentle till-covered slopes of the south sides of the Kalguty Valley, west of the Central Valley fan, mainly from 2400 to 2600 m.

Block streams, i.e. linear deposits of coarse debris along hillslopes (Wilson, 2013), are abundant on the east side of the Klyuch Valley. They are most likely relict features and had developed on gradients in the range 7.5–15°. Openwork clasts showing a roughly inverse grading are angular (a few presenting a slight edge-rounding), covered by lichens, and mostly in the range 10–50 cm in length at the surface. At half slope, 1- to 2-m-wide block streams occupy shallow depressions, but clasts overlain by the thick meadow on the margins suggest a continuation of debris beyond the lateral apparent limits (Figure 6(b)) – as observed elsewhere (Wilson, 2013). Indeed, as a downslope extension to broad blockfields and block slopes related to the rock outcrops on the top of the hill, block streams have a braided/anastomosing plan form uphill. Block stream formation combined several processes (stripping, frost creep and wedging, gelifluction) over a long period (Wilson, 2013).

Few small solifluction stone-banked lobes (i.e. lobate sorted accumulations; Benedict, 1970) are present on the 3050 m plateau (Figure 6(d)). On the other hand, larger turf-banked lobes and terraces (i.e. lacking conspicuous sorting) are active for instance on the Klyuch

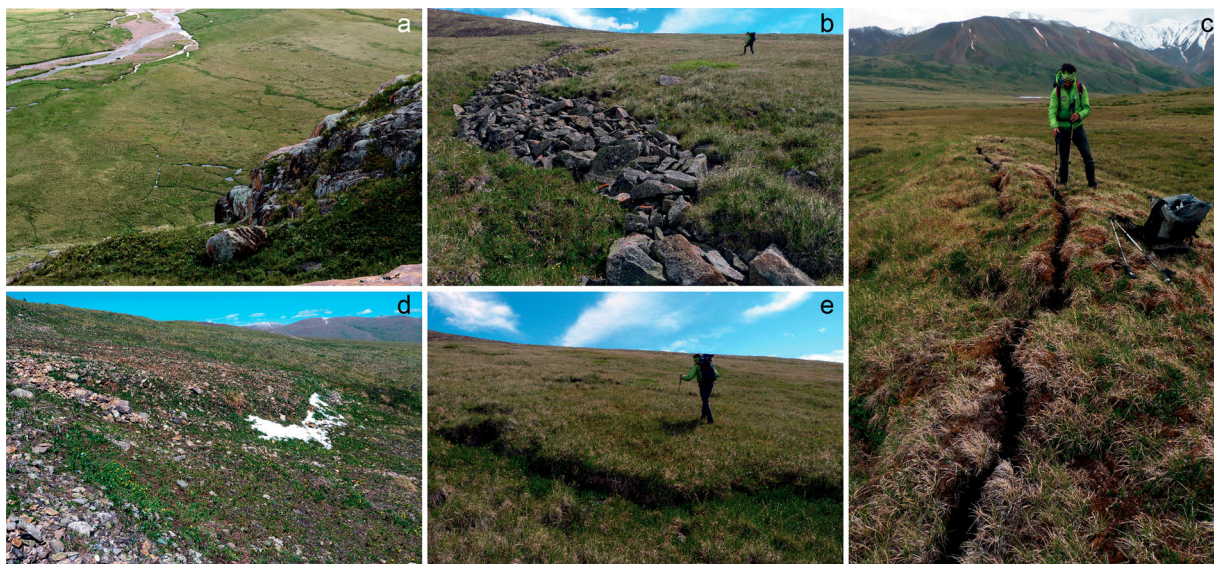


**Figure 6.** Periglacial landforms. (a) Ice-wedge polygons in alluvial deposit at the foot of Kalgutinski Rudnik; Kalguty river in the background; (b) block stream on the Klyuch Valley east side; (c) narrow trough in a ridge inside the Klyuch morainic complex, possibly due to seasonal frost cracking; (d) 0.3-m-high stone-banked gelifluction lobe on the 3050 m plateau; (e) 0.5-m-high turf-banked gelifluction lobe in the Klyuch Valley.

valley east side (Figure 6(e)). As measured in other mountain ranges, displacement affects the surficial ground (<1 m depth) with a rate of few  $\text{cm.yr}^{-1}$ , since solifluction results from the combination between (i) seasonal and diurnal frost creep (limited in turf-banked lobes) driven by frost heaving and slope angle, and (ii) gelifluction, i.e. the translational movement induced by micro-slipping along ice lens boundaries, enhanced by water from snowmelt and precipitation (Kinnard & Lewkowicz, 2005).

Talus sheets and cones located south to Kalguty river supply or supplied debris to a protalus rampart and rock glaciers. A protalus rampart is a ridge of coarse clasts that results from falling, sliding, bouncing or rolling of rock debris across a perennial snowbank to accumulate at its margin (Wilson, 2009). A 200-m-long one with outer and inner flanks c. 15- and 5-m-high, respectively, is located at 2730 m asl in the Central Valley (Figure 7(c)), as suggested by the c. 50-m wide depression between the crest and the talus foot upslope, the slope angle of the potential snowbank ( $30^\circ$ ), and the absence of rock-slope failure at the top of the talus

(Ballantyne & Benn, 1994). The absence of a snowbank at the beginning of July suggests that this protalus rampart is now relict.

Rock glaciers are more abundant in the basin. A lobate or tongue-shaped accumulation of ice and angular clasts, a rock glacier has sub-concentric ridges and furrows on its surface bowed outward in the direction of motion, and a steep (c.  $40^\circ$ ) and sharply defined front when active. Talus-derived rock glaciers have a high content of ice (40–70%), in the form of interstitial ice, and ice lenses and strata: besides ice segregation, the supersaturated ice body forms from snow banks and avalanche snow deposits recovered by debris (Berthling, 2011). A large rock glacier complex is located in the Central Valley cirque (Figure 7(b)). Its main body (RG1) is inactive nowadays, as suggested by the fuzzy contact at 2850 m asl between its steep 60-m-high front with the downstream debris flow deposits, and by the patchy vegetation and the roughly sorted polygons on its top. RG1 is no longer connected to upstream large polygenic cones that result from debris/rockfalls, debris flows and snow avalanching.



**Figure 7.** Talus-related landforms. (a) Inactive and fossil rock glaciers in the Tundu-Uqgar Valley (c. 2670 m asl); (b) rock glacier complex in the Central cirque, seen from the opposite side of the Kalguty Valley (front: c. 2850 m); (c) protalus rampart in the Central Valley (2730 m); on the left: part of an alluvial cone.

Moisture in the fine-grained sediments along its left margin could indicate water seepage from melting of the internal ice, possibly also expressed by the depression formed by the 8-m-high reverse slope upstream of the RG1 top. An alternative hypothesis is that debris source for RG1 included the slope below the small east crest that stretches between 3000 and 3100 m; then, the ‘right latero-frontal moraines’ would have been the margins of RG1 when active.

Upstream, a 350-m-long rock glacier (RG2) is separated from RG1 by a narrow trough drained by snow meltwater. The upper section of this active RG2 is contained between the foot of the talus slope and the frontal moraines built by a former glacier. RG1 and RG2 are tongue-shaped rock glaciers (Wahrhaftig & Cox, 1959). A 350-m-wide, short and lobate RG3 is located at the bottom of the cirque headwall, connected to the talus sheet. It could have formed in recent decades, because of the current uphill shift of the permafrost distribution: between 2007 and 2016, mountain permafrost warmed on average by  $0.19 \pm 0.05$  °C (Biskaborn et al., 2019). No longer connected to the talus sheet but still active, RG2 is likely in thermal disequilibrium with the current climate.

Inactive or fossil rock glaciers are numerous from the south side of the West Valley to the east side of the Tundu-Uqgar Valley (Figure 7(a)). The tongue-shaped rock glacier in the West Valley is still connected to active polygenic cones but is likely to be inactive (front <2600 m). In the Tundu-Uqgar Valley, rock glaciers, generally short and lobate, extend at the foot of the slope along 2 km, with front elevations in the range 2650–2850 m. They are inactive or even partly fossil as suggested by a double front (overlapping), vegetated flat areas, a dominant low slope angle of the frontal slopes, and deep gullying; some fresher ridges on the upper part of a tongue-shaped rock glacier located upstream suggest that it could be still active. Small creeping features on the talus sheet of the valley’s upper section possibly indicate past/recent buried ice, in permafrost condition. In the lower section of the Tundu-Uqgar Valley, several coalescent,

short tongue-shaped rock glaciers are located at the bottom of the talus sheet with fronts at 2655–2680 m. Steep fronts, vegetation on wide flat areas, or active talus cones covering the rock glaciers without creeping evidence suggest inactive landforms, whereas fully vegetated smooth ridges indicate fossil rock glaciers (Figure 7(a)).

Small fossil rock glaciers are also present. Inactive lobate rock glaciers with fronts at c. 2730–2740 m are located at the bottom of a steep, northwest-facing slope between the West and Central Valleys. In the Central Valley, a chaotic set of few pronounced, partly vegetated ridges corresponds to a former lobate rock glacier whose front reached 2680 m asl; a fresher small ridge at its top suggests a local reactivation, possibly as protalus rampart. Finally, two 400-m-wide, short and lobate rock glaciers partly vegetated with front at 2720–2730 m are located at the north-eastern end of the 3050 m plateau; a close tongue-shaped one whose front reached 2640 m is nowadays largely buried by clasts from an active talus cone.

In spite of low annual precipitation, summer snow patches and firn fields on the highest slopes of the headwalls of Tundu-Uqgar and Central Valleys (Figure 8) suggest that steep slopes are affected by spring snow avalanches that can reach low elevations when channelized in a gully (Figure 8(b)). The geomorphic role of snow avalanching is revealed by abundant clasts at the surface of the rare avalanche deposits in July, resulting from the scouring of the gully sides. It is also illustrated by the smooth and regular surface of many talus cones, where large clasts are reworked and transported downstream (Figures 5(b) and 8(b)). Snow avalanching combines with torrential processes, boulder fall and rockfall in the funnel-shaped mixed basins.

On the other hand, snow patches lying in the Kalguty Valley bottom between the main lake and the confluence (2410–2430 m asl; Figure 3(a)) and in the Ulan-Dawa river bed (2505–2525 m; Figure 4(a)), whose summer duration varies each year, are not snow avalanche deposits. Like other apparent snow patches on satellite images located on the stream bed and lakes at the end of spring, these ‘snow patches’

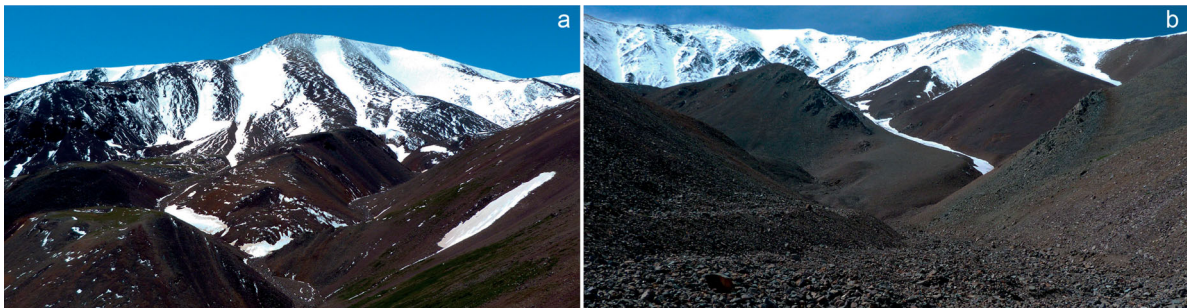


**Figure 8.** Snow avalanching. (a) Snow patches and firn fields on the headwalls of the Tundu-Uqgar Valley above c. 3000 m asl (early July); (b) fresh snowfall on the crests and snow avalanche deposit (front: c. 2820 m) in the central gully of the Central Valley; scoured surface of debris cone by snow avalanching in the centre of the image; active stream channel in the foreground.

are actually remnants of icings/aufeis, i.e. layered sheets of ice formed during winter from ground water seepage or stream discharge (Hu & Pollard, 1997; Pavelsky & Zarnetske, 2017). Active groundwater discharge is attested to in summer by the numerous peat bogs distributed on the lower, gentler slopes of the valley. Unlike the thick meadow that covers the rest of the valley bottom, the ground underlying the icings outside stream beds is poorly or non-vegetated due to their duration, with numerous clasts at its surface.

### 4.3. Mass movements

Few landslide deposits are observed in the upper Kalguty basin: these are mainly small rockfall and rock slide deposits in the Tundu-Uqgar Valley. An earth flow could have affected a slope along one of the northern tributaries of the Ulan-Dawa river. Developed on a c. 200 m vertical drop, its vegetated deposit suggests it has been inactive for a long time. Another potential mass movement is located between the West and the Central Valleys, downstream of the inactive rock glaciers; its chaotic but vegetated surface suggests an old event, may be a rock slide. The most remarkable landslide feature of the study area is the deformation of the lower kame terrace on the north side of the Kalguty Valley: according to the position of its downstream section compared to the upper kame terrace, the 2.4-km-long main section of the lower terrace has slid by 30–90 m vertically and 100–450 m along the slope. Areas of maximal deformation are in relation with the surficial drainage network. Finally, large paraglacial rock-slope failures have not been observed.

### 4.4. Fluvial processes and landforms

Surface runoff on the north side of the Kalguty Valley mainly concentrates in rills and small gullies in a dominant parallel drainage pattern. Some deeper gullies breach the kame terraces and allow the formation of small alluvial cones, generally associated with slope peat bogs. By contrast, the steep and elevated south side is characterized by the dendritic patterns of deeply incised Argamji, West, Central, and Tundu-Uqgar Valleys (Figure 2), and few individual gullies. Longitudinal profiles of these valley streams are gentle (e.g. the average gradient of the Central river is 11°), with no nick-points. Once the snow cover has largely melted out, summer discharge of the valley rivers is limited. However, up to 40–60-m-wide active braided channels with cobbles and boulders, and local erosion of banks indicate that high peak discharge occurs annually (Figure 8 (b)). Wider inactive channels resulted from recent lateral migration of the streams, especially onto the large alluvial fans on the Kalguty Valley floor. The absence of an alluvial fan downstream of the Tundu-Uqgar valley is due to the sediment trapping in the large floodplain

dammed by the inner moraines. A smaller alluvial cone is located at the confluence between the Central river and one of its tributaries (Figure 7(c)).

The anastomosing channel of the Kalguty river presents a high degree of anabranching due to frequent avulsions as shown by satellite images, and favoured by its low gradient. It is filled with coarse pebbles and cobbles while some of its islands are partly vegetated, and flanked by a wider inactive channel covered by meadow – generally, a wetland drained by a dense network of former river branches. Finally, low alluvial terraces are present all along the valley bottom. They are especially extensive along the Ulan-Dawa river, downstream of the Central alluvial fan, and upstream of the western morainic complex. Lakes distributed along the valley bottom could correspond to kettles resulting from the melting of ice pieces once buried in the glacial melt-out till.

## 5. Conclusions

The broad geomorphic analysis illustrates the contrast between both sides of the permafrost-affected upper Kalguty Valley. The north side is still entirely covered by tills and many lateral moraines and kame terraces whereas the south side is mainly affected by periglacial processes. In more detail, the south side shows a rough altitudinal zonation: tills affected by patterned ground dominate up to c. 2700 m asl, above which regolith covers the upper slopes as talus sheets and cones, blockfields and block slopes, and supplies/supplied rock glaciers. Lower gentle slopes of the valley are prone to peat bog formation and locally present likely relict block streams. Finally, the valley bottom is infilled by alluvial deposits interstratified with the alluvial fans built by the torrential deposits from the south steep side.

Markers of past glacier extents are better preserved on the valley bottom and the gentle lower slopes, mainly in the form of morainic complexes, erratic boulders, and roches moutonnées like the Kalgutinski Rudnik. As yet no ages are available for these glacial landforms. The western morainic complex is considered to be LGM by Blomdin et al. (2014). Klyuch, Tundu-Uqgar and Central complexes would therefore have been built during the Lateglacial, while the most upstream moraines in the Tundu-Uqgar and Central Valleys could correspond to the LIA glacier extent. This relative glacial chronology will be further constrained by ongoing surface exposure dating at Kalgutinski Rudnik, and completed by a detailed archeo-geomorphological survey of this site.

### Software

Mapping was conducted using QGIS (2.18.16), with final editing carried out with Adobe Illustrator CC 2018.

## Acknowledgements

Estelle Ployon, Cécile Pignol, Laura Poiriel, and Xavier Bodin (EDYTEM) made the field topographic map background and the SPOT DEM. Fieldwork in Altai was funded by the LIA Multidisciplinary Research on Prehistoric Art in Eurasia – ARTEMIR. The authors acknowledge the three reviewers, John Abraham, Iestyn Barr, and Peter Wilson, whose relevant suggestions contributed in improving the map and paper quality, and the English. The authors thank Martin Kirkbride for having reviewed the English.

## Disclosure statement

No potential conflict of interest was reported by the author(s).

## Funding

This work was supported by public funds received in the framework of GEOSUD which supplied the SPOT6/7 and Pléiades images, a project (ANR-10-EQPX-20) of the program 'Investissements d'Avenir' managed by the French National Research Agency.

## References

- Ballantyne, C. K. (2010). A general model of autochthonous blockfield evolution. *Permafrost and Periglacial Processes*, 21(4), 289–300. <https://doi.org/10.1002/ppp.700>
- Ballantyne, C. K. (2018). *Periglacial geomorphology* (472 p.). Wiley-Blackwell.
- Ballantyne, C. K., & Benn, D. I. (1994). Glaciological constraints on proglacial rampart development. *Permafrost and Periglacial Processes*, 5(3), 145–153. <https://doi.org/10.1002/ppp.3430050304>
- Batbaatar, J., Gillespie, A. R., Fink, D., Matmon, A., & Fujioka, T. (2018). Asynchronous glaciations in arid continental climate. *Quaternary Science Reviews*, 182, 1–19. <https://doi.org/10.1016/j.quascirev.2017.12.001>
- Benedict, J. B. (1970). Downslope soil movement in a Colorado Alpine region: Rates, processes and climatic significance. *Arctic and Alpine Research*, 2(3), 165–226. <https://doi.org/10.1080/00040851.1970.12003576>
- Berthling, I. (2011). Beyond confusion: Rock glaciers as cryo-conditioned landforms. *Geomorphology*, 131(3–4), 98–106. <https://doi.org/10.1016/j.geomorph.2011.05.002>
- Biskaborn, B. K., Smith, S. L., Noetzi, J., Matthes, H., Vieira, G., Streletskiy, D. A., Schoeneich, P., Romanovsky, V. E., Lewkowicz, A. G., Abramov, A., Allard, M., Boike, J., Cable, W. L., Christiansen, H. H., Delaloye, R., Diekmann, B., Drozdov, D. S., Etzelmüller, B., Grosse, G., ... Lantuit, H. (2019). Permafrost is warming at a global scale. *Nature Communications*, 10(1), 11. <https://doi.org/10.1038/s41467-018-08240-4>
- Black, R. F. (1976). Periglacial features indicative of permafrost: Ice and soil wedges. *Quaternary Research*, 6, 3–26. [https://doi.org/10.1016/0033-5894\(76\)90037-5](https://doi.org/10.1016/0033-5894(76)90037-5)
- Blomdin, R., Heyman, J., Stroeven, A. P., Hättestrand, C., Harbor, J. M., Gribenski, N., Jansson, K. N., Petrakov, D. A., Ivanov, M. N., Alexander, O., Rudoy, & A. N., Walther, M. (2014). Glacial geomorphology of the Altai and western Sayan mountains, central Asia. *Journal of Maps*, 12, 123–136. <https://doi.org/10.1080/17445647.2014.992177>
- Chandler, B. M. P., Lovell, H., Boston, C. M., Lukas, S., Barr, I. D., Benediktsson, ÍÖ, Benn, D. I., Clark, C. D., Darvill, C. M., Evans, D. J. A., Ewertowski, M. W., Loibl, D., Margold, M., Otto, J.-C., Roberts, D. H., Stokes, C. R., Storrar, R. D., & Stroeven, A. P. (2018). Glacial geomorphological mapping: A review of approaches and frameworks for best practice. *Earth-Science Reviews*, 185, 806–846. <https://doi.org/10.1016/j.earscirev.2018.07.015>
- Chikisheva, T. A., Polosmak, N. V., & Zubova, A. V. (2015). The burial at Ak-Alakha-3 Mound 1, Gorny Altai: New findings. *Archaeology, Ethnology and Anthropology of Eurasia*, 43(1), 144–154. <https://doi.org/10.1016/j.aeae.2015.07.016>
- Ganiushkin, D., Chistyakov, K., Volkov, I. V., Bantsev, D. V., Kunaeva, E., & Terekhov, A. V. (2017). Present glaciers and their dynamics in the arid parts of the Altai mountains. *Geosciences*, 7(4), 117. <https://doi.org/10.3390/geosciences7040117>
- Gorbunov, A. P., Marchenko, S. S., & Seversky, E. V. (2004). The thermal environment of blocky materials in the mountains of Central Asia. *Permafrost and Periglacial Processes*, 15(1), 95–98. <https://doi.org/10.1002/ppp.478>
- Guodong, C., Yuanming, L., Zhizhong, S., & Fan, J. (2007). The 'thermal semi-conductor' effect of crushed rocks. *Permafrost and Periglacial Processes*, 18(2), 151–160. <https://doi.org/10.1002/ppp.575>
- Hu, X., & Pollard, W. H. (1997). Ground icing formation: Experimental and statistical analyses of the overflow process. *Permafrost and Periglacial Processes*, 8(2), 217–235. [https://doi.org/10.1002/\(SICI\)1099-1530\(199732\)8:2<217::AID-PPP251>3.0.CO;2-1](https://doi.org/10.1002/(SICI)1099-1530(199732)8:2<217::AID-PPP251>3.0.CO;2-1)
- Kinnard, C., & Lewkowicz, A. G. (2005). Movement, moisture and thermal conditions at a Turf-banked Solifluction Lobe, Kluane Range, Yukon Territory, Canada. *Permafrost and Periglacial Processes*, 16(3), 261–275. <https://doi.org/10.1002/ppp.530>
- Lachenbruch, A. H. (1962). Mechanics of thermal contraction cracks and Ice-wedge polygons in permafrost. *Geological Society of America Special Paper*, 70, 65. <https://doi.org/10.1130/SPE70>
- Mackay, J. R. (1974). Ice-wedge cracks, Garry Island, north-west Territories. *Canadian Journal of Earth Sciences*, 11(10), 1366–1383. <https://doi.org/10.1139/e74-133>
- Mackay, J. R. (1990). Some observations on the growth and deformation of epigenetic, syngenetic, and antisynthetic ice wedges. *Permafrost and Periglacial Processes*, 1(1), 15–29. <https://doi.org/10.1002/ppp.3430010104>
- Marchenko, S., Ishikawa, M., Sharkhuu, N., Jin, H., Li, X., Lin, Z., Yabuki, H., & Brown, J. (2006). *Distribution and monitoring of Permafrost in Central and Eastern Asia* (Workshop on Permafrost of Central and Eastern Asia Report). 4 p.
- Matsuoka, N., & Murton, J. (2008). Frost weathering: Recent advances and future directions. *Permafrost and Periglacial Processes*, 19(2), 195–210. <https://doi.org/10.1002/ppp.620>
- Molodin, V. I., & Cheremisin, D. V. (2007). Petroglyphs of the Ukok Plateau. *Archaeology, Ethnology and Anthropology of Eurasia*, 32(1), 91–101. <https://doi.org/10.1134/S1563011007040081>
- Molodin, V. I., Polosmak, N. V., Novikov, A. V., Bogdanov, E. S., Slyusarenko, I. Y., & Cheremisin, D. V. (2004). Archaeological sites of the Ukok Plateau (Gorny Altai). IAE SO RAN. *Materialy po arkheologii Sibiri*, 3, 256. p. (in Russian).
- Murton, J. B., Peterson, R., & Ozouf, J. C. (2006). Bedrock fracture by ice segregation in cold regions. *Science*, 314(5802), 1127–1129. <https://doi.org/10.1126/science.1132127>
- Pavelsky, T. M., & Zarnetske, J. P. (2017). Rapid decline in river icings detected in Arctic Alaska: Implications for a changing hydrologic cycle and river ecosystems.

- Geophysical Research Letters*, 44(7), 3228–3235. <https://doi.org/10.1002/2016GL072397>
- Peel, M. C., Finlayson, B. L., & McMahon, T. A. (2007). Updated world map of the Köppen-Geiger climate classification. *Hydrology and Earth System Sciences*, 11(5), 1633–1644. <https://doi.org/10.5194/hess-11-1633-2007> doi:10.5194/hess-11-1633-2007
- RGI Consortium. (2017). Randolph glacier Inventory (RGI) – A Dataset of Global glacier Outlines: Version 6.0. Technical Report, Global Land Ice Measurements from Space, Boulder. *Digital Media*, <https://doi.org/10.7265/N5-RGI-60>
- Riseborough, D., Shiklomanov, N., Etzelmüller, B., Gruber, S., & Marchenko, S. (2008). Recent advances in permafrost modeling. *Permafrost and Periglacial Processes*, 19(2), 137–156. <https://doi.org/10.1002/ppp.615>
- Rudoy, A. N. (2002). Glacier-dammed lakes and geological work of glacial superfloods in the Late Pleistocene, southern Siberia, Altai mountains. *Quaternary International*, 87(1), 119–140. [https://doi.org/10.1016/S1040-6182\(01\)00066-0](https://doi.org/10.1016/S1040-6182(01)00066-0)
- Sass, O., & Krautblatter, M. (2007). Debris flow-dominated and rockfall-dominated talus slopes: Genetic models derived from GPR measurements. *Geomorphology*, 86(1–2), 176–192. <https://doi.org/10.1016/j.geomorph.2006.08.012>
- Shahgedanova, M., Nosenko, G., Khromova, T., & Muraveyev, A. (2010). Glacier shrinkage and climatic change in the Russian Altai from the mid-20th century: An assessment using remote sensing and PRECIS regional climate model. *Journal of Geophysical Research Atmospheres*, 115(D16), D16107. <https://doi.org/10.1029/2009JD012976>
- Wahrhaftig, C., & Cox, A. (1959). Rock glaciers in the Alaska Range. *Geological Society of America Bulletin*, 70(4), 383–436. [https://doi.org/10.1130/0016-7606\(1959\)70\[383:RGITAR\]2.0.CO;2](https://doi.org/10.1130/0016-7606(1959)70[383:RGITAR]2.0.CO;2)
- Washburn, A. L. (1973). *Periglacial processes and environments* (320 p.). Arnold.
- Wilson, P. (2009). Rockfall talus slopes and associated talus-foot features in the glaciated uplands of Great Britain and Ireland: Periglacial, paraglacial or composite landforms? In J. Knight, & S. Harrison (Eds.), *Periglacial and paraglacial processes and environments* (pp. 133–164). Geological Society of London.
- Wilson, P. (2013). Block/rock streams. In S. A. Elias, & C. J. Mock (Eds.), *Encyclopedia of Quaternary Science* (pp. 514–522). Elsevier.